

# Revision of absorption corrections for the $pp \rightarrow pp\pi^+\pi^-$ process

Piotr Lebiedowicz\* and Antoni Szczurek †‡

*Institute of Nuclear Physics PAN, PL-31-342 Kraków, Poland*

## Abstract

We include new additional absorption corrections into the Lebiedowicz-Szczurek (non-resonant) model for  $pp \rightarrow pp\pi^+\pi^-$  or  $p\bar{p} \rightarrow p\bar{p}\pi^+\pi^-$  processes. They are related to the  $\pi N$  nonperturbative interaction in the final state of the reaction. The role of the absorption corrections is quantified for several differential distributions for  $\sqrt{s} = 0.2, 1.96, 7$ , and  $8$  TeV. The new absorption corrections lead to further decrease of the cross section by about a factor of two. They change the shape of some distributions ( $d\sigma/dt$ ,  $d\sigma/dp_{t,p}$ ,  $d\sigma/d\phi_{pp}$ ) but leave almost unchanged shape of other distributions ( $d\sigma/dM_{\pi\pi}$ ,  $d\sigma/dy_{\pi}$ ,  $d\sigma/dp_{t,\pi}$ ,  $d\sigma/d\phi_{\pi\pi}$ ). The effect may have important impact on the interpretation of the recent STAR and CDF data as well as the forthcoming data of the ALICE, ATLAS + ALFA and CMS + TOTEM collaborations.

PACS numbers: 12.40.Nn, 13.60.Le, 14.40.Be

---

† Also at University of Rzeszów, PL-35-959 Rzeszów, Poland.

\*Electronic address: Piotr.Lebiedowicz@ifj.edu.pl

‡Electronic address: Antoni.Szczurek@ifj.edu.pl

## I. INTRODUCTION

There is a growing experimental and theoretical interest in understanding of soft hadronic processes at high energy; for reviews see e.g. [1–3] and references therein. One of the reaction which can be relatively easy to measure is  $pp \rightarrow p\pi^+\pi^-p$  or  $p\bar{p} \rightarrow p\pi^+\pi^-\bar{p}$  (four charged particles in the final state). There are recently several experimental projects by the COMPASS [4, 5], STAR [6], CDF [7, 8], ALICE [9, 10], ATLAS [11], and CMS [12] collaborations which will measure differential cross sections for the reaction(s). Here we wish to compare predictions from the Lebedowicz-Szczurek model with the recent STAR and CDF data.

The principal reason for studying central exclusive production of mesons is to search for glueballs [13]. There is some evidence from an analysis of the decay modes of the scalar states observed, that the lightest scalar glueball manifests itself through the mixing with nearby  $q\bar{q}$  states [14, 15]. The exclusive production of lower mass scalar and pseudoscalar resonances within a tensor pomeron approach [16] was recently examined in [17]. Resonant ( $\rho^0 \rightarrow \pi^+\pi^-$ ) and non-resonant (Drell-Söding) photon-pomeron/Reggeon production was studied in [18]. In Refs. [19, 20] the continuum background to the production of the  $\chi_c(0^+)$  state via two-body  $\pi^+\pi^-$  and  $K^+K^-$  decays was considered. For exclusive production of other mesons see e.g. [21–23], where mainly the non-central processes were discussed.

Some time ago we proposed a simple phenomenological model for the  $\pi^+\pi^-$ -continuum mechanism [see diagrams in Fig. 1 (a)] using the tools of Regge theory [24], where perturbative QCD cannot be reliably applied. In this model the parameters of pomeron and subleading reggeon exchanges were adjusted to describe total and elastic  $\pi N$  scattering. We expect that our parametrization correctly extrapolate the interaction parameters to higher energies where there are no experimental data. The non-resonant model can be supplemented to include the  $pp$  or  $p\bar{p}$  absorption effects [2, 19]; see diagrams in Fig. 1 (b). The largest uncertainties in the Lebedowicz-Szczurek model are due to the unknown off-shell pion form-factor and the absorption corrections (the soft survival factor due to screening corrections). The absorption is done in the eikonal approximation. The absorption effects lead to substantial damping of the cross section. The damping depends on the collision energy and kinematical variables. The discussed here model, with reasonable vertex form factors accounting for off-shellness of non-pion-like pions in the middle of diagrams in Fig. 1, gives a rough description of the ISR data [25–27]. To get a reasonable description of existing so far experimental data parameter(s) of the form factors has (have) to be adjusted [2, 19].

It is not clear if the considered so far absorption effects are sufficient to describe the

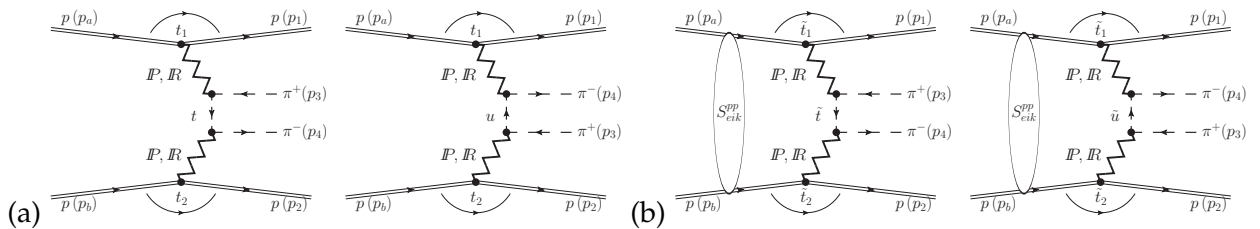


FIG. 1: (a) Born amplitudes for the  $pp \rightarrow pp\pi^+\pi^-$  process. (b) Absorptive correction amplitudes due to the  $pp$  interaction.

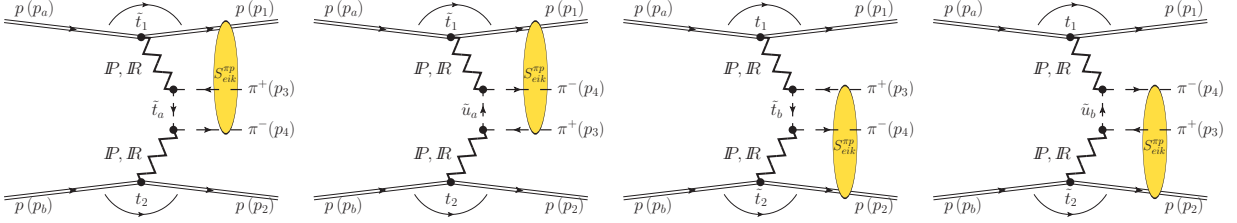


FIG. 2: New absorptive correction amplitudes for the  $pp \rightarrow pp\pi^+\pi^-$  process due to the  $\pi p$  interaction in the final state included in the present analysis.

data. Any interaction between participating particles potentially leads to absorptive effects, as it destroys exclusivity of the process. In Fig. 1 (b) we show schematically absorptive amplitudes due to  $\pi N$  interaction in the final state. Not all combination of interactions are shown in the figure. Some absorptive effects are included inherently in our calculation; by using effective interaction fitted to describe  $\pi N$  elastic scattering data.

Recently, the Lebedowicz-Szczurek model [24] was implemented in GenEx MC [28]. There absorptive corrections are not taken into account explicitly. The authors of [29] constructed a DIME Monte Carlo code, where almost the same approach was implemented. In [29] a two-channel eikonal model was considered.

In the present paper we will include the additional absorptive effects, not considered so far in the literature, and quantify their role for total cross section and for many differential distributions for the considered process. Our theoretical results will be compared to recent experimental results obtained by the STAR [6] and CDF [7, 8] collaborations. We will also show some predictions for ALICE, ATLAS and CMS experiments.

## II. BORN AMPLITUDE

The amplitude squared for the  $pp \rightarrow pp\pi^+\pi^-$  process (with four-momenta  $p_a + p_b \rightarrow p_1 + p_2 + p_3 + p_4$ ) considered within the framework of Regge theory with the central  $\pi^+\pi^-$  system produced by the exchange of two pomeron/reggeon in the  $t$ -channel, as shown in Fig. 1, can be written as

$$|\mathcal{M}|^2 = |\mathcal{M}_{I=0}|^2 + |\mathcal{M}_{I=1}|^2 + |\mathcal{M}_{I=2}|^2, \quad (2.1)$$

where the isospin amplitudes can be decomposed to the Regge ingredients as

$$\mathcal{M}_{I=0} = \mathcal{M}^{PP} + \mathcal{M}^{Pf_{2R}} + \mathcal{M}^{f_{2R}P} + \mathcal{M}^{f_{2R}f_{2R}} + \langle 1,0;1,0 | 0,0 \rangle \mathcal{M}^{\rho R \rho R}, \quad (2.2)$$

$$\mathcal{M}_{I=1} = \mathcal{M}^{P\rho R} + \mathcal{M}^{\rho R P} + \mathcal{M}^{f_{2R}\rho R} + \mathcal{M}^{\rho R f_{2R}}, \quad (2.3)$$

$$\mathcal{M}_{I=2} = \langle 1,0;1,0 | 2,0 \rangle \mathcal{M}^{\rho R \rho R}. \quad (2.4)$$

The Clebsch-Gordan coefficients  $\langle j_1, m_1; j_2, m_2 | j, m \rangle$  are

$$\langle 1,0;1,0 | 0,0 \rangle = \sqrt{2/3} \quad \text{and} \quad \langle 1,0;1,0 | 2,0 \rangle = -\sqrt{1/3}.$$

The situation can be summarized as

$$|\mathcal{M}_{I=0}|^2 \gg |\mathcal{M}_{I=1}|^2 \gg |\mathcal{M}_{I=2}|^2. \quad (2.5)$$

For the dominant pomeron-pomeron contribution we have C-parity  $C = +1$  and isospin  $I = 0$  of the produced  $\pi^+\pi^-$  system. In general, not only leading double pomeron exchanges contribute, but also the subleading  $f_{2R}$  ( $C = +1$ ) and  $\rho_R$  ( $C = -1$ ) reggeon exchanges.<sup>1</sup>

The Born amplitude with the intermediate pion exchange can be written as

$$\mathcal{M}_{pp \rightarrow pp\pi^+\pi^-}^{\text{Born}} = M_{13}(s_{13}, t_1) \frac{F_\pi^2(t)}{t - m_\pi^2} M_{24}(s_{24}, t_2) + M_{14}(s_{14}, t_1) \frac{F_\pi^2(u)}{u - m_\pi^2} M_{23}(s_{23}, t_2) \quad (2.6)$$

where the subsystem amplitudes  $M_{ij}(s_{ij}, t_i)$  denotes “interaction” between forward proton ( $i = 1$ ) or backward proton ( $i = 2$ ) and one of the two pions ( $j = 3$  for  $\pi^+$  or  $j = 4$  for  $\pi^-$ ). The energy dependence of the  $\pi p$  subsystem amplitudes  $M_{ij}$  is parametrised in terms of the pomeron and the  $f_{2R}$  reggeon exchange

$$M_{ij}(s_{ij}, t_i) = \eta_P s_{ij} C_P^{\pi N} \left( \frac{s_{ij}}{s_0} \right)^{\alpha_P(t_i)-1} \exp \left( \frac{B_P^{\pi N}}{2} t_i \right) + \eta_{f_{2R}} s_{ij} C_{f_{2R}}^{\pi N} \left( \frac{s_{ij}}{s_0} \right)^{\alpha_{f_{2R}}(t_i)-1} \exp \left( \frac{B_{f_{2R}}^{\pi N}}{2} t_i \right), \quad (2.7)$$

where  $\eta_P = i$ ,  $\eta_{f_{2R}} = -0.860895 + i$ ,  $s_{ij}$  is the energy in the  $(ij)$  subsystem, and the energy scale  $s_0$  is fixed at  $s_0 = 1 \text{ GeV}^2$ . The pomeron and reggeon trajectories,  $\alpha_P(t)$  and  $\alpha_{f_{2R}}(t)$ , respectively, are assumed to be of standard form, see for instance [30], that is, linear in  $t$ :

$$\alpha_P(t) = \alpha_P(0) + \alpha'_P t, \quad \alpha_P(0) = 1.0808, \quad \alpha'_P = 0.25 \text{ GeV}^{-2}, \quad (2.8)$$

$$\alpha_{f_{2R}}(t) = \alpha_{f_{2R}}(0) + \alpha'_{f_{2R}} t, \quad \alpha_{f_{2R}}(0) = 0.5475, \quad \alpha'_{f_{2R}} = 0.93 \text{ GeV}^{-2}. \quad (2.9)$$

We found the slope parameters  $B_{P/f_{2R}}^{\pi N}$  from fitting the elastic  $\pi^+ p$  and  $\pi^- p$  cross sections

$$B_P^{\pi N} = 5.5 \text{ GeV}^{-2}, \quad B_{f_{2R}}^{\pi N} = 4 \text{ GeV}^{-2}. \quad (2.10)$$

Our model makes various simplifications, but describes the data for elastic  $\pi N$  scattering fairly well for energies  $\sqrt{s_{\pi N}} \gtrsim 2.5 \text{ GeV}$  (see Fig. 2.2 of [2]).

So far we have assumed a simple exponential dependence of the  $\pi N$  subprocess amplitudes (2.7) which is valid only for small  $|t|$  ( $0.01 < -t < 0.4 \text{ GeV}^2$ ). At larger  $|t|$  ( $t_1$  or  $t_2$  in the  $2 \rightarrow 4$  case) the mechanism becomes more complicated. Here a subsequent exchange of two pomerons and the exchange of the pomeron together with the reggeon,

---

<sup>1</sup> The  $\rho_R \rho_R$  component is negligible (see the strength parameters in Table 2.1 of [2]) and was omitted in our analysis. We emphasize, that at lower energies (COMPASS, ISR) the subleading  $f_{2R}$  exchanges constitute a large contribution to the total cross section and must be included in addition to the pomeron exchanges; see e.g. section 2.3 of [2]. Furthermore, there is a large interference effect between the different components in the amplitude of about 50% (the total cross section in full phase space), see section 2.6.2 of [2]. As we shall see in the results section imposing limitations on pion rapidity  $|y_\pi| < 1$  and going to higher energies reduces the role of subleading  $f_{2R}$  exchanges, however, due to their non-negligible interference effects with the leading  $PP$  term we keep them explicitly in our calculations.

or even pQCD effects (two-gluon exchange) may show up.<sup>2</sup> To give a more realistic  $t$  dependence we suggest the following replacement (see also [36])

$$\exp\left(\frac{B_P^{\pi N}}{2} t_i\right) \left(\frac{s_{ij}}{s_0}\right)^{\alpha'_P t_i} \rightarrow f(t_i, s_{ij}) = \exp\left(\mu^2 B(s_{ij})\right) \exp\left(-\mu^2 B(s_{ij}) \sqrt{1 - \frac{t_i}{\mu^2}}\right);$$

$$B(s_{ij}) = B_0 + 2\alpha'_P \ln\left(\frac{s_{ij}}{s_0}\right), \quad (2.11)$$

where the free parameters  $\mu$ ,  $B_0$  has been adjusted to the  $\pi N$  elastic scattering data, as illustrated in Fig. 3. The so-called ‘stretched exponential’ parametrization  $f(t_i, s_{ij})$  coincides at low  $|t|$  with the simple exponential form while at larger  $|t|$  features a harder tail. This function is close to a parametrization  $\sim \exp(-bp_\perp)$  suggested by Orear [37] for elastic  $pp$ -scattering. The  $\pi p$  data show a diffraction dip at  $-t \sim 4 \text{ GeV}^2$ .

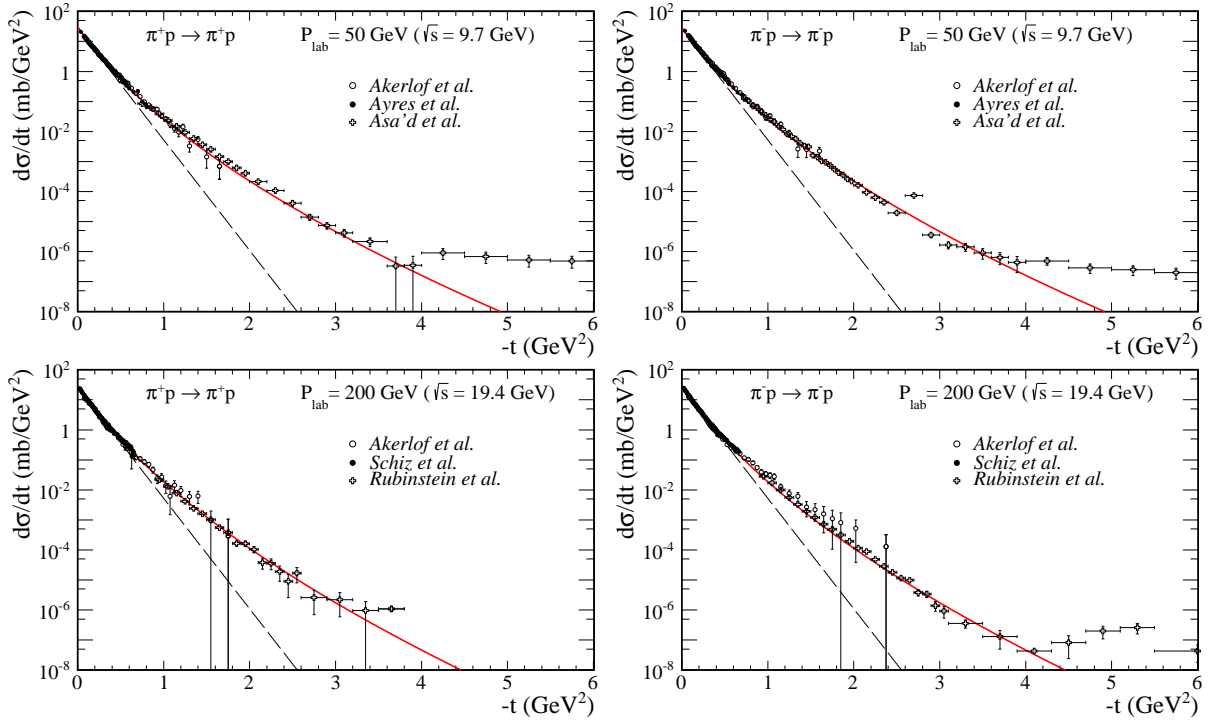


FIG. 3: Differential distributions  $d\sigma/dt$  for  $\pi^+p$  (left panel) and  $\pi^-p$  (right panel) elastic scattering at incident beam momenta  $P_{lab} = 50 \text{ GeV}$  ( $\sqrt{s} \simeq 9.7 \text{ GeV}$ ) [38–40] and  $P_{lab} = 200 \text{ GeV}$  ( $\sqrt{s} \simeq 19.4 \text{ GeV}$ ) [38, 41, 42]. The black dashed lines show results with formula (2.10) while the red solid lines are obtained via the replacement (2.11), where  $B_0 = 6.5 \text{ GeV}^{-2}$  and  $\mu^2 = 0.6 \text{ GeV}^2$ .

The extra form factors  $F_\pi(t)$  and  $F_\pi(u)$ , in Eq. (2.6), “correct” for the off-shellness of the intermediate pions. The form of the form factor is unknown in particular at higher values

<sup>2</sup> Even description of the elastic  $pp$  and  $p\bar{p}$  scattering data is difficult. In Ref. [31] the authors present a model including  $P + PP + ggg$  terms and the linear pomeron trajectory. Alternative approaches [32, 33] combine the soft and hard pomeron exchanges or the odderon exchange in addition [34]. In the latter case the authors consider also a various forms of the non-linear pomeron trajectory. In [35] the role of the eikonalization of the  $pp$  amplitude in both one- and the two-channel eikonal models were discussed.

of  $t$  or  $u$  and they are parametrised in two ways:

$$F_\pi(t) = \exp\left(\frac{t - m_\pi^2}{\Lambda_{off,E}^2}\right), \quad (2.12)$$

$$F_\pi(t) = \frac{\Lambda_{off,M}^2 - m_\pi^2}{\Lambda_{off,M}^2 - t} \quad (2.13)$$

and for  $F_\pi(u)$  we have to replace  $t \longleftrightarrow u$ . These form factors are normalized to unity on the pion-mass-shell  $F_\pi(m_\pi^2) = 1$ . In general, the parameter  $\Lambda_{off}$  is not known precisely but, in principle, could be fitted to the normalized experimental data. How to extract the off-shell parameters will be discussed in the Result section.

### III. ABSORPTION CORRECTIONS

So far only absorption effects due to  $pp$  ( $p\bar{p}$ ) interactions were included in the literature in the calculations of cross sections for the  $pp \rightarrow pp\pi^+\pi^-$  ( $p\bar{p} \rightarrow p\bar{p}\pi^+\pi^-$ ) reactions [2, 19]. Here we wish to include also the absorption effects due to strong nonperturbative interaction of charged pions and (anti)protons in the final state, see corresponding diagrams in Fig. 2). The absorption amplitude including the  $\pi N$  interactions can be written in a similar way as that in the case of  $pp$  ( $p\bar{p}$ ) interaction, i.e., in the eikonal form

$$\begin{aligned} \mathcal{M}_{pp \rightarrow pp\pi^+\pi^-}^{\pi p\text{-rescattering}} \approx & \frac{i}{16\pi^2 s_{14}} \int d^2 k_t \mathcal{M}_{pp \rightarrow pp\pi^+\pi^-}^{\text{Born}}(s, \tilde{t}_1, t_2, \tilde{t}_a) \mathcal{M}_{\pi^- p \rightarrow \pi^- p}^{P\text{-exchange}}(s_{14}, k_t^2) \\ & + \frac{i}{16\pi^2 s_{13}} \int d^2 k_t \mathcal{M}_{pp \rightarrow pp\pi^+\pi^-}^{\text{Born}}(s, \tilde{t}_1, t_2, \tilde{u}_a) \mathcal{M}_{\pi^+ p \rightarrow \pi^+ p}^{P\text{-exchange}}(s_{13}, k_t^2) \\ & + \frac{i}{16\pi^2 s_{23}} \int d^2 k_t \mathcal{M}_{pp \rightarrow pp\pi^+\pi^-}^{\text{Born}}(s, t_1, \tilde{t}_2, \tilde{t}_b) \mathcal{M}_{\pi^+ p \rightarrow \pi^+ p}^{P\text{-exchange}}(s_{23}, k_t^2) \\ & + \frac{i}{16\pi^2 s_{24}} \int d^2 k_t \mathcal{M}_{pp \rightarrow pp\pi^+\pi^-}^{\text{Born}}(s, t_1, \tilde{t}_2, \tilde{u}_b) \mathcal{M}_{\pi^- p \rightarrow \pi^- p}^{P\text{-exchange}}(s_{24}, k_t^2). \quad (3.1) \end{aligned}$$

In formula (3.1) we have indicated explicitly only crucial variables, mostly those arguments of  $\mathcal{M}_{pp \rightarrow pp\pi^+\pi^-}$  which get modified in comparison to the Born amplitude (2.6). For example, the four-momenta squared of the Regge exchange in the first stage of the interaction (see Fig. 2) get modified as

$$\tilde{t}_1 = (\tilde{p}_1 - p_a)^2, \quad \tilde{t}_2 = (\tilde{p}_2 - p_b)^2, \quad (3.2)$$

where the four-momenta of the intermediate nucleons are  $\tilde{p}_1 = p_1 - k_t$  and  $\tilde{p}_2 = p_2 - k_t$ . Here, we have introduced auxiliary four-vector  $k_t = (0, \vec{k}_t, 0)$  to write formulas in a compact way. Similarly, the modified four-momenta of pions being propagated in the middle of the four-body  $pp \rightarrow pp\pi^+\pi^-$  subprocess can be calculated as

$$\begin{aligned} \tilde{t}_a &= (\tilde{q}_1 - p_3)^2, & \tilde{u}_a &= (\tilde{q}_1 - p_4)^2, \\ \tilde{t}_b &= (\tilde{q}_2 - p_4)^2, & \tilde{u}_b &= (\tilde{q}_2 - p_3)^2, \end{aligned} \quad (3.3)$$

where  $\tilde{q}_1 = p_a - \tilde{p}_1$  and  $\tilde{q}_2 = p_b - \tilde{p}_2$  are the four-momenta of the (incoming) Regge exchanges. We leave all other not explicitly indicated variables which appear in the Born

amplitude(s) unchanged. This is an approximation but sufficient for the purpose of the present first exploratory analysis.

The full amplitude includes all rescattering corrections

$$\mathcal{M}_{pp \rightarrow pp\pi^+\pi^-} = \mathcal{M}_{pp \rightarrow pp\pi^+\pi^-}^{\text{Born}} + c_{pp}\mathcal{M}_{pp \rightarrow pp\pi^+\pi^-}^{pp\text{-rescattering}} + c_{\pi p}\mathcal{M}_{pp \rightarrow pp\pi^+\pi^-}^{\pi p\text{-rescattering}}. \quad (3.4)$$

In principle the contributions due to the intermediate proton(s) diffractive excitation(s) ( $p \rightarrow N^*$ ) could be effectively included by increasing the prefactors. In the present paper we shall take, however,  $c_{pp} = c_{\pi p} = 1$ .<sup>3</sup>

In the next section we shall show effect of inclusion of the extra absorption terms on total cross section as well as on differential distributions. They will lead to further decrease of the cross section for the  $pp \rightarrow pp\pi^+\pi^-$  or  $p\bar{p} \rightarrow p\bar{p}\pi^+\pi^-$  reactions. We expect that the effects may be very important when comparing results of our calculation with the recent STAR and CDF experimental data as well as with the forthcoming data of the ALICE, CMS, and ATLAS collaborations.

#### IV. PREDICTIONS FOR DIFFERENT EXPERIMENTS

In this section we shall present some selected results for the discussed exclusive processes calculated for kinematic domains relevant for the STAR, CDF, ALICE, CMS, and ATLAS experiments. In particular, we wish to concentrate on the effect of the new absorption corrections due to the pion-(anti)proton interaction. We refer also the readers to section 2.6.2 of [2] where only the absorptive corrections due to  $NN$  interaction were discussed.

Before we go to the higher energies let us first discuss old ISR data [25, 27]. In Fig. 4 (top panels) we show results for two-pion invariant mass distributions. The theoretical calculations including absorption corrections have been compared with the ISR data. In the calculation the form factor for the off-shell pions was fixed as specified in the figure captions. The choice of form factor leads to different behaviour at higher  $M_{\pi\pi}$ . We also show (bottom panels) the result for the exponential and 'stretched exponential'  $t$ -dependences without and with absorption corrections. The shape of the  $t$  distributions is strongly modified by the absorption corrections and is similar as obtained in the ISR experiment.

##### A. STAR experiment

In Fig. 5 we present the invariant mass distributions of the pion pair produced in the  $pp \rightarrow pp\pi^+\pi^-$  reaction for the STAR kinematics ( $\sqrt{s} = 200$  GeV,  $|\eta_\pi| < 1$  and  $p_{t,\pi} > 0.15$  GeV for both pions, the pseudorapidity of the central  $\pi^+\pi^-$  system  $|\eta_{\pi\pi}| < 2$ , and in the four-momentum transfers range  $0.005 < -t_1, -t_2 < 0.03$  GeV<sup>2</sup>). In the left panel we show result obtained in the Born approximation (dotted line), the result when including proton-proton interactions (dashed line), and when including extra pion-nucleon interactions discussed in the present paper. We observe significant damping

---

<sup>3</sup> How the extra multiplication of the absorption amplitude  $\mathcal{M}_{pp \rightarrow pp\pi^+\pi^-}^{pp\text{-rescattering}}$  by a factor  $c_{pp} = 1.2$  modify the features of differential distributions was shown in [2], see, e.g., Figs. 2.48, 2.49, 2.50, and Table 2.5.

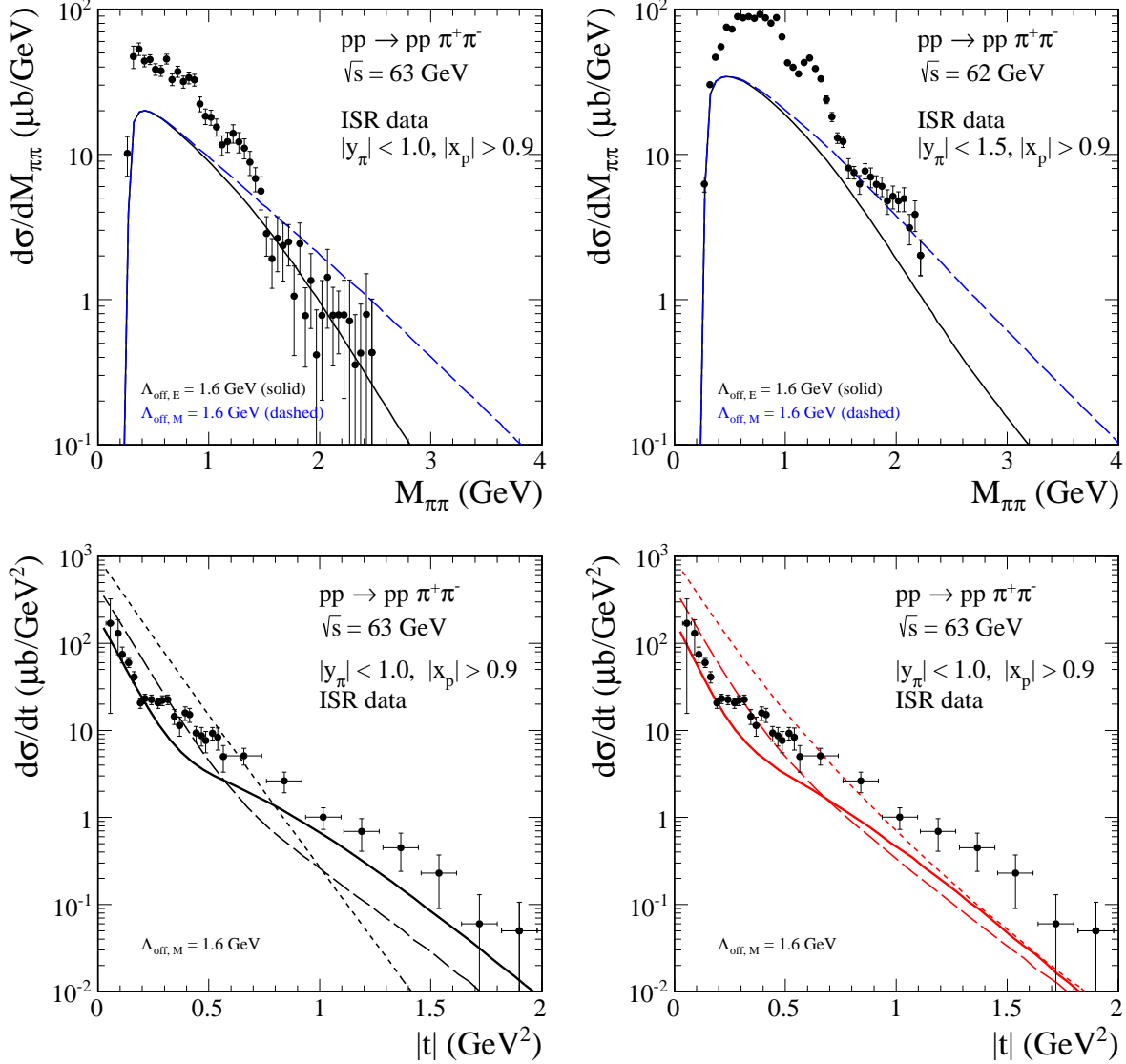


FIG. 4: Two-pion invariant mass distribution at ISR energies with the ISR kinematical cuts indicated in the figure caption. The ISR data [25, 27] are shown for comparison. The blue dashed lines represent the results obtained for the monopole form factors [(2.13),  $\Lambda_{off,M} = 1.6$  GeV], while the black solid lines are for the exponential form [(2.12),  $\Lambda_{off,E} = 1.6$  GeV]. The bottom panels represent the  $|t|$  distributions without (dotted lines), with the  $pp$  absorption corrections (dashed lines), and with all ( $pp$  and  $\pi N$ ) absorption corrections included (solid lines). Results for the exponential (left bottom panel) and for the ‘stretched exponential’ (right bottom panel) parametrizations of the  $\pi p$  subsystem are shown.

of the cross section as well as a small shift of the maximum towards smaller invariant masses. In the left panel we show result for different parameters of the off-shell form factors, together with the STAR experimental data. One can observe that our predictions are quite sensitive to the form of the off-shell pion form factor (2.12) or (2.13) and depend on the value of the cut-off parameters  $\Lambda_{off}$ . If we describe the maximum of the cross section around  $M_{\pi\pi} \sim 0.6-0.7$  GeV we overestimate the cross section in the interval  $1 <$



$M_{\pi\pi} < 2$  GeV essentially for both choices of the form factor form. Part of the effect may be related to an enhancement of the cross section due to  $\pi\pi$  low-energy final state interaction. This goes beyond the scope of the present paper which concentrates on the new absorption effects.

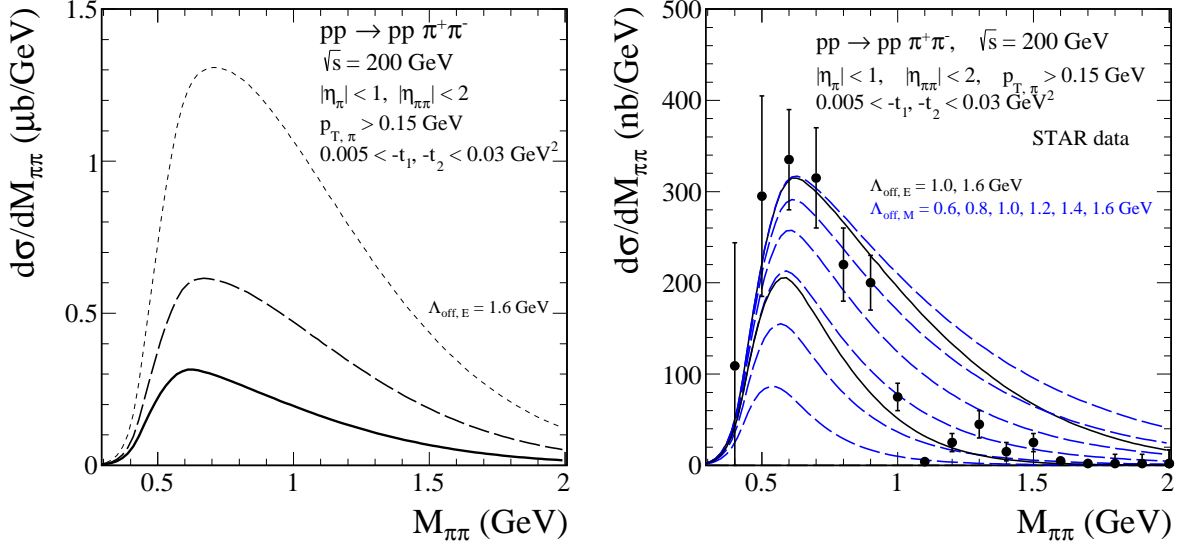


FIG. 5: Two-pion invariant mass distribution at  $\sqrt{s} = 200$  GeV with the STAR kinematical cuts specified in the figure caption. The dotted line in the left panel corresponds to the Born calculation, the long-dashed and solid lines to calculations with the absorption effects due to the  $pp$ - and the  $\pi p$ -rescattering in addition, respectively. In the right panel, the blue dashed lines represent the results with all absorption effects and obtained for the monopole form factors (2.13) for different choices of the cut-off parameter  $\Lambda_{\text{off},M} = 0.6$ -1.6 GeV (from bottom to top). The black solid lines are for the exponential form (2.12) and  $\Lambda_{\text{off},E} = 1.0$  and  $1.6$  GeV. The STAR data [6] are shown for comparison.

In Fig. 6 (left panel) we show differential cross section for the exclusive production of  $\pi^+\pi^-$  system as a function of its pseudorapidity. We conclude that in the range  $0.5 < M_{\pi\pi} < 1.0$  GeV both forms of the off-shell pion form factor [(2.12) and (2.13)] describe the data well for  $\Lambda_{\text{off}} = 1.4 - 1.6$  GeV. However, the agreement seems a bit misleading in the light of disagreement in the invariant mass distribution discussed above. As will be discussed in this paper, the absorption effects usually strongly modify the distribution in relative azimuthal angle between the outgoing protons  $\phi_{pp}$  and leave the shape of the  $\phi_{\pi\pi}$  distribution almost unchanged. For the STAR (Phase I) visible kinematical range, that is at very small four-momentum transfers  $|t|$ , one can observe only a damping of the cross section (the right bottom panel). The decrease of  $d\sigma/d\phi_{pp}$  and  $d\sigma/d\phi_{\pi\pi}$  at  $\phi \sim \pi$  is due to the condition  $|\eta_{\pi\pi}| < 2$ .

## B. CDF experiment

We wish to emphasize that in this experiment, in contrast to the STAR experiment, the final-state nucleons are not detected and only rapidity gap conditions ( $\Delta\eta > 4.6$  on

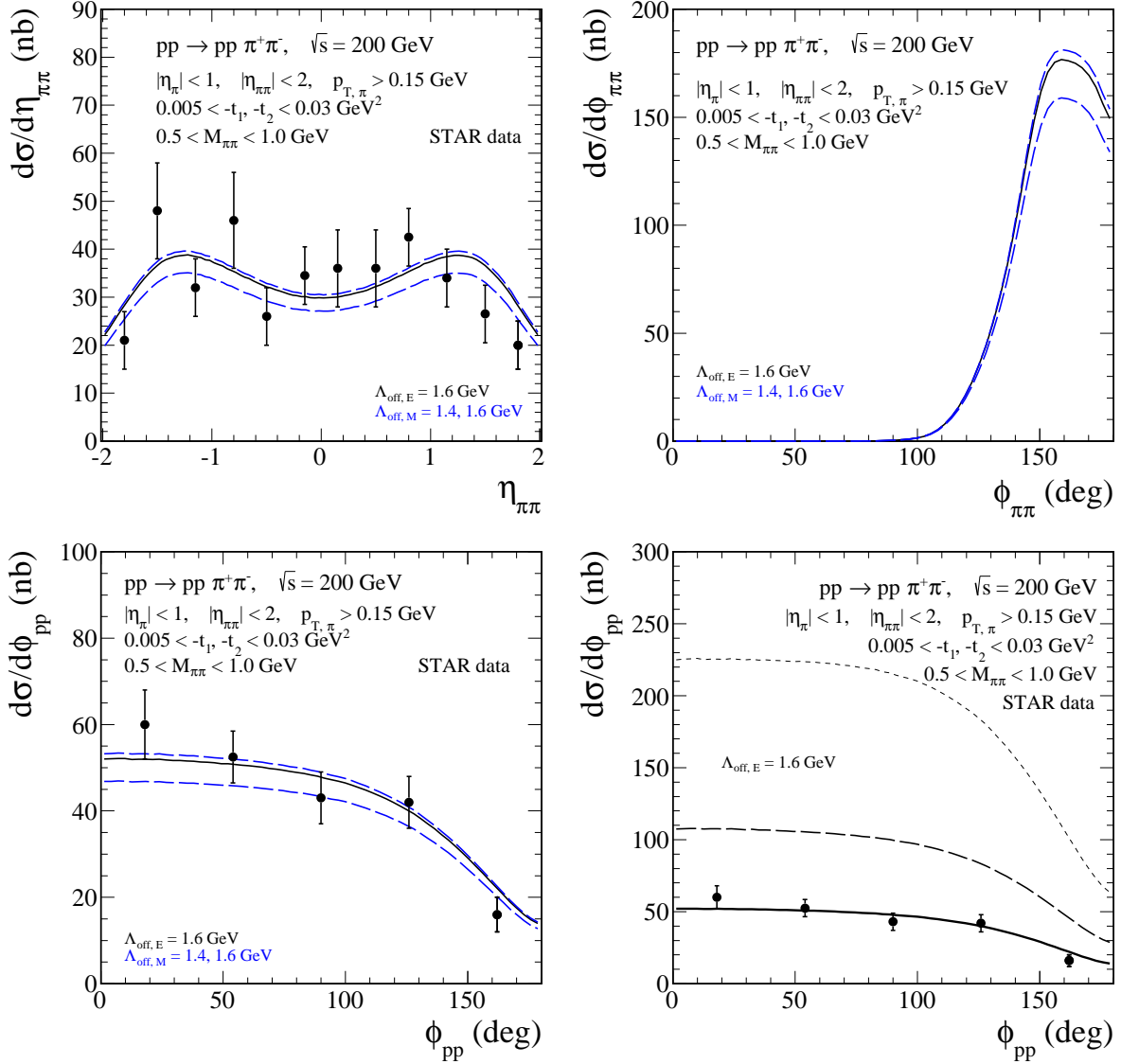


FIG. 6: The distributions in the pseudorapidity of the produced  $\pi^+\pi^-$  system ( $\eta_{\pi\pi}$ ) and in the azimuthal angle between the outgoing pions ( $\phi_{\pi\pi}$ ) and between the outgoing protons ( $\phi_{pp}$ ) at  $\sqrt{s} = 200$  GeV in the range of  $0.5 < M_{\pi\pi} < 1.0$  GeV. In the right bottom panel we show the results without the absorption effects (the dotted line), with the  $pp$ -rescattering (the long-dashed line), and with the additional  $\pi p$ -rescattering (the solid line). The STAR data [6] are shown for comparison.

each side of the  $\pi^+\pi^-$ ) was imposed experimentally. In Fig. 7 we show the two-pion invariant mass distribution at  $\sqrt{s} = 1.96$  TeV for the  $p\bar{p} \rightarrow p\bar{p}\pi^+\pi^-$  reaction and with the following CDF cuts on kinematical variables:  $p_{t,\pi} > 0.4$  GeV,  $|\eta_\pi| < 1.3$  for both mesons, and  $|y_{\pi\pi}| < 1$ . The rapidity of the central  $\pi^+\pi^-$  system is expressed by the formula

$$y_{\pi\pi} = \frac{1}{2} \ln \left( \frac{(p_{30} + p_{40}) + (p_{3z} + p_{4z})}{(p_{30} + p_{40}) - (p_{3z} + p_{4z})} \right), \quad (4.1)$$

with the four-momenta  $p_3$  ( $\pi^+$  meson) and  $p_4$  ( $\pi^-$  meson). The kinematical cuts  $p_{t,\pi} > 0.4$  GeV on both pions strongly distort the region of low  $M_{\pi\pi} < 1$  GeV. At  $M_{\pi\pi} \simeq 1$  GeV the data show a minimum due to interference of the  $f_0(980)$  resonance contribution with the non-resonant background contribution. At higher  $M_{\pi\pi}$ , in the region of 1.2-1.7 GeV, some structures could be attributed to  $f_2(1270)$ ,  $f_0(1370)$ ,  $f_0(1500)$ , and  $f_0(1710)$  resonant states. The  $f_0(1500)$  and the  $f_0(1710)$  mesons are considered to be scalar glueball candidates [14], but mixing with quarkonium states complicating the issue. We roughly describe the differential cross section in the left panel when using the form factors (2.13) with  $\Lambda_{off,M} \simeq 0.8$  GeV. The data at  $\sqrt{s} = 0.9$  TeV look similar (see Fig. 1 of [8]). The data at both energies include diffractive dissociation of proton and antiproton (all the produced unobserved hadrons have  $|\eta| > 5.9$ ), so that low diffractive masses of the baryonic systems are included, especially at  $\sqrt{s} = 1.96$  TeV. In the right panel of Fig. 7 we show results with an extra cut on the  $\pi^+\pi^-$  transverse momentum. The results for the form factors that give a reasonable description in the left panel badly fail to describe the data in the right panel, underestimating the CDF data by a factor of about 5. In this case our model results are much below the experimental data which could be due to a contamination of non-exclusive processes or the perturbative mechanism discussed in [20]. Both the interference of resonant state with the  $\pi^+\pi^-$ -continuum and the diffractive dissociation effects require more subtle theoretical approach. This will be addressed elsewhere. Thus, the non-resonant Lebiedowicz-Szczurek model should not be expected to fit the data precisely. We conclude that the CDF data for  $p_{t,\pi\pi} > 1$  GeV [8] are sensitive to the details of the “large”- $t$  behavior of the  $\pi N$  scattering. While neglecting the extra  $\pi N$  absorptive corrections the stretched exponential functional form gives larger cross section than the standard exponential form, however, the inclusion of the extra  $\pi N$  absorption cancels the “improvement”. In this moment we do not know a solution of this puzzle.

Now let us discussed shortly quantities or observables that are sensitive to the pion off-shell form factors. The dependence of  $\langle p_{t,\pi} \rangle$  and  $\langle p_{t,\pi\pi} \rangle$  as a function of two-pion invariant mass is presented in Fig. 8. Our calculation shows a rise of the average pion transverse momentum with dipion invariant mass. A dependence on the form of the form factor is clearly seen. On the contrary, the average transverse momentum of the dipion pair is almost independent of the form of the form factor and a parameter of the form factor. This can be understood from momentum conservation. The transverse momentum of the dipion system must be balanced by the transverse momenta of protons. The latter distributions (shapes) are obviously independent of the pion off-shell form factors.

Another observable which can be very sensitive to the choice of off-shell pion form factors are the Legendre polynomials  $\langle P_{Leven}(\cos \theta_{\pi^+}^{r.f.}) \rangle (M_{\pi\pi})$  distributions, where  $\cos \theta_{\pi^+}^{r.f.}$  is the angle of the  $\pi^+$  meson with respect to the beam axis, in the  $\pi^+\pi^-$  rest frame. In Fig. 9 we present the average  $P_L$  calculated as

$$\langle P_L(\cos \theta_{\pi^+}^{r.f.}) \rangle (M_{\pi\pi}) = \frac{\int d\mathcal{PS} P_L(\cos \theta_{\pi^+}^{r.f.}) d\sigma/d\mathcal{PS}(M_{\pi\pi})}{\int d\mathcal{PS} d\sigma/d\mathcal{PS}(M_{\pi\pi})}, \quad (4.2)$$

where the integral is done over experimental phase space. We have found that the  $\langle P_L(\cos \theta_{\pi^+}^{r.f.}) \rangle (M_{\pi\pi})$  distributions are almost unaffected by the absorption effects. The difference between the results for form factors (2.12) and (2.13) is huge at higher invariant masses and thus such observables may prove very useful in distinguishing

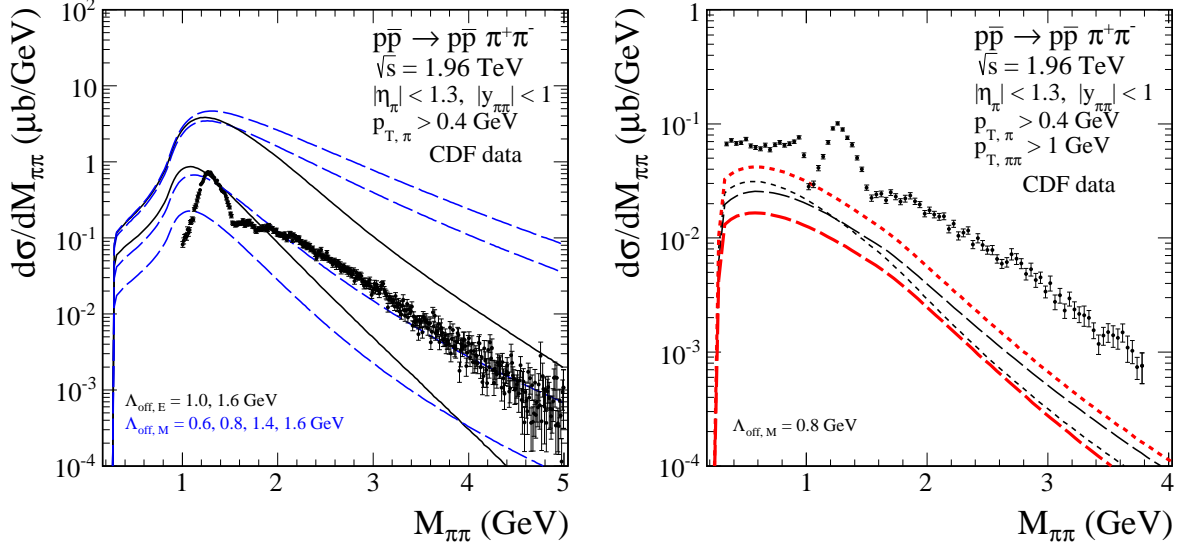


FIG. 7: Two-pion invariant mass distribution at  $\sqrt{s} = 1.96$  TeV with the CDF kinematical cuts specified in the figure caption. The meaning of the lines in the left panel is the same as in Fig. 5. In the right panel we show the results with an additional cut on transverse momentum of the pair  $p_{T,\pi\pi} > 1$  GeV without (dotted lines) and with (long-dashed lines) the  $\pi N$  absorption corrections and for two different  $t$ -dependences of the  $\pi p$ -subsystem amplitudes. The black thin lines show results with formula (2.10) while the red thick lines represent results for the replacement (2.11) ( $B_0 = 6.5 \text{ GeV}^{-2}$ ,  $\mu^2 = 0.6 \text{ GeV}^2$ ). The CDF data [7, 8] are shown with only statistical errors; systematic uncertainties are approximately 10% at all masses.

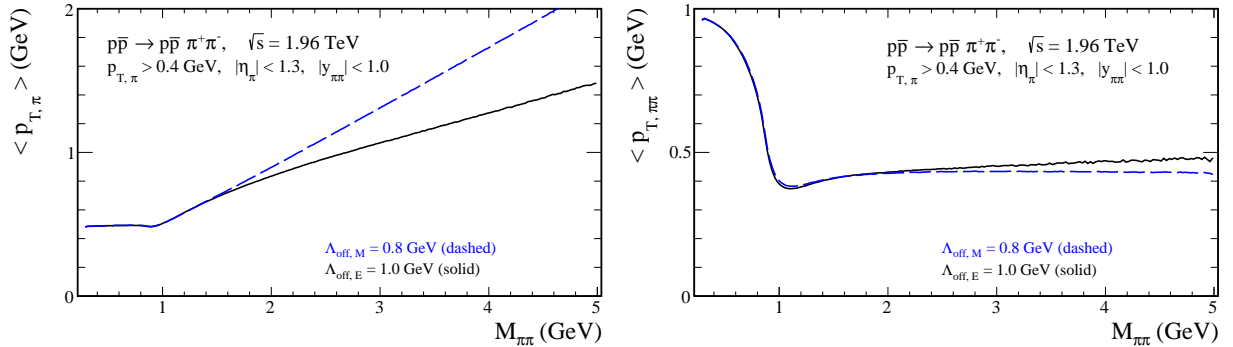


FIG. 8: Mean value of  $p_{T,\pi}$  (left panel) and  $p_{T,\pi\pi}$  (right panel) as a function of two-pion invariant mass at  $\sqrt{s} = 1.96$  TeV calculated with the CDF kinematical cuts specified in the figure caption.

between these choices. Experimental results of the  $\langle P_L(\cos\theta_{\pi^+\pi^-}^{r.f.}) \rangle (M_{\pi\pi})$  distributions for  $\sqrt{s} = 1.96$  TeV are presented in Fig. 23 of [7] and strongly support our predictions calculated with the monopole form factors (2.13) and the cut-off parameter  $\Lambda_{off,M} = 0.8$  GeV, particularly at higher two-pion invariant masses  $M_{\pi\pi} > 1.5$  GeV; see also discussion in section 2.6.2 (Tevatron) of [2]. One can observe in Fig. 2.42 of [2] that the contribution of  $L = 4$  is small at low  $M_{\pi\pi}$  when the cuts are neglected (left panels) and significant already at  $M_{\pi\pi} \approx 1$  GeV when the cuts are applied (right panels). This

suggests that the CDF kinematic cuts may distort the partial wave content. This makes conclusions more difficult.

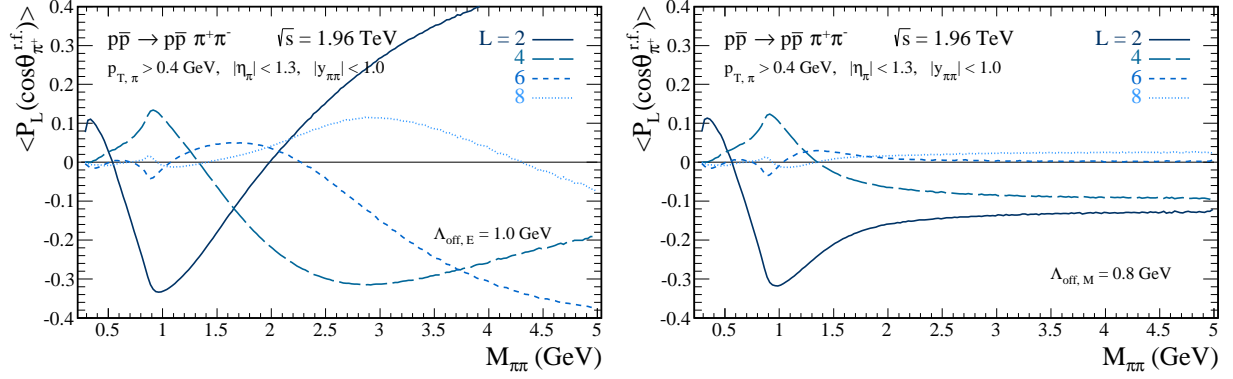


FIG. 9: Mean value of the first even Legendre polynomials  $P_L(\cos \theta_{\pi^+ \pi^-}^{r.f.})$  as a function of two-pion invariant mass with the CDF kinematical cuts specified in the figure caption. The results correspond to two types of off-shell pion form factors: the exponential one (2.12) and the monopole one (2.13).

### C. ALICE experiment

Now, we shall present our predictions for experiments at the LHC. We shall start review of our results for the case of the ALICE experiment at  $\sqrt{s} = 7$  TeV. We impose the corresponding cuts on both pions transverse momenta  $p_{t,\pi} > 0.1$  GeV and pseudorapidities  $|\eta_\pi| < 0.9$ . In Fig. 10 we show two-pion invariant mass distribution. As for the case of the STAR experiment in the left panel we show the Born result (dotted line), the result with  $pp$  absorption only (dashed line) as well as the results when including the extra  $\pi p$  absorption (solid line). There is similar tendency as for the STAR case. The extra absorption lower the cross section without modifying the shape of the invariant mass distribution. In the right panel we show our result for two different forms of the off-shell form factor and different values of the cut-off parameters. As for the STAR case the shape strongly depends on the form factor form as well as on the cut-off parameters.

Now we pass to distributions in transverse momenta of single pion and of the pion pair, see Fig. 11 (top panels). The absorption effects due to  $\pi p$  interaction change the shape of the  $p_{t,\pi\pi}$ -distribution. Such a distribution can be easily measured by the ALICE collaboration. The ALICE experiment cannot register forward/backward protons. Therefore only azimuthal correlations between pions can be measured. Our corresponding distribution is shown in Fig.11 (bottom panel). The  $\phi_{\pi\pi}$  distribution peaks in the back-to-back configuration, i.e. when  $\phi_{\pi\pi} = \pi$ . The absorption effects practically do not change the shape of the distributions.

The average values of transverse momenta of single pion  $\langle p_{t,\pi} \rangle (M_{\pi\pi})$  and of the pion pair  $\langle p_{t,\pi\pi} \rangle (M_{\pi\pi})$  are shown in Fig. 12. The results have been obtained assuming that  $p_{t,\pi} > 0.1$  GeV without the absorption effects (the dotted line), with the  $pp$ -rescattering (the long-dashed line), and with the additional  $\pi p$ -rescattering (the solid line).

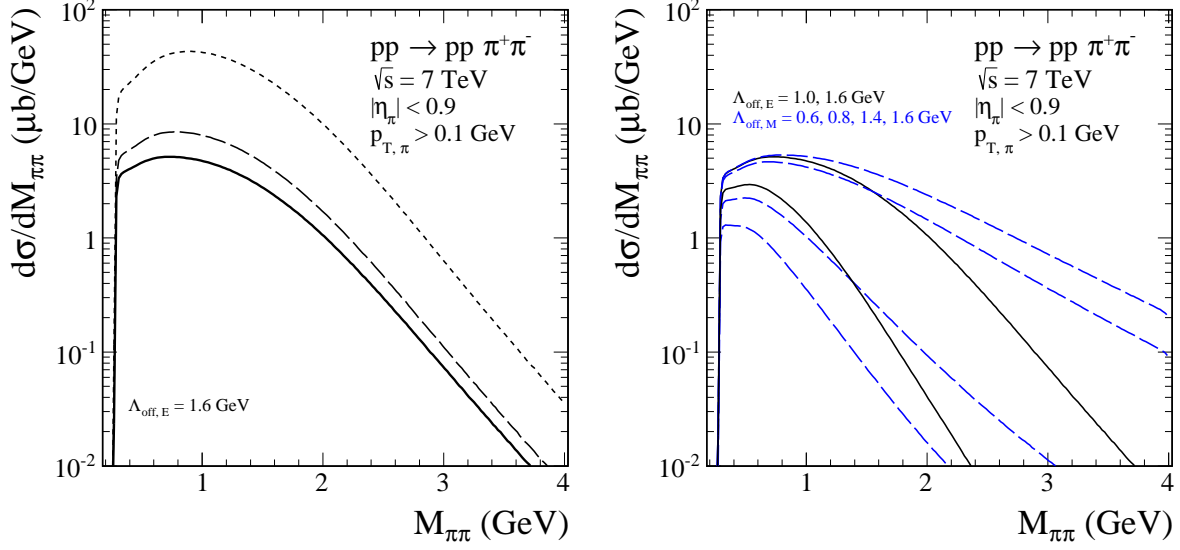


FIG. 10: Two-pion invariant mass distribution at  $\sqrt{s} = 7$  TeV with the ALICE kinematical cuts specified in the figure caption. In the left panel we show results with a cut-off parameter  $\Lambda_{off,E} = 1.6$  GeV, see (2.12), without the absorption effects (the dotted line), with the  $pp$ -rescattering (the long-dashed line), and with the additional  $\pi p$ -rescattering (the solid line). The meaning of the lines in the right panel is the same as in Fig. 5.

#### D. CMS and ATLAS experiments

The ATLAS tracking detector provides measurement of charged particle momenta in the  $|\eta| < 2.5$  region. Since the correlation between the pseudorapidities of both pions is very large, the measurement can be performed independently using the tracking detector ( $|\eta| < 2.5$ ) and the forward calorimeters ( $2.5 < |\eta| < 4.9$ ), see Fig. 4 of [11]. We wish to note that the analysis in [11] was performed for  $\Lambda_{off,E}^2 = 2$  GeV<sup>2</sup> neglecting effect of the  $\pi N$  rescattering. Below we shall show results of non-resonant model (including all rescattering corrections) for the CMS experiment and the corresponding kinematics cuts on both pions:  $p_{t,\pi} > 0.1$  GeV and  $|\eta_\pi| < 2.0$ . The general features of the differential distributions for the ATLAS experiment are, however, similar.

In Fig. 13 we show two-pion invariant mass distribution. In the left panel we show again results for three cases: Born (dashed line), absorption due to  $pp$  interaction (dashed line) and for the case with extra  $\pi p$  interaction (solid line). In the right panel we show the dependence of the cross section on the choice of the pion off-shell form factor.

Both the CMS (when combined with TOTEM) and ATLAS (when combined with ALFA) collaborations can measure outgoing protons. What additional information can be provided by measuring the momenta of the outgoing protons? In Figs. 14 and 15 we show the influence of the absorption effects on the  $p_{t,p}$ ,  $\phi_{pp}$ , and  $t$  distributions. The distribution in proton transverse momenta are particularly interesting. The extra absorption effects due to  $\pi p$  interactions make the distributions much broader than in the case of Born approximation and even broader than in the case when only  $pp$  absorption effects are included. The effect depends on the value of cut-off parameter  $\Lambda_{off}$ . Therefore we expect that the CMS and ATLAS experimental groups could verify our predictions. The

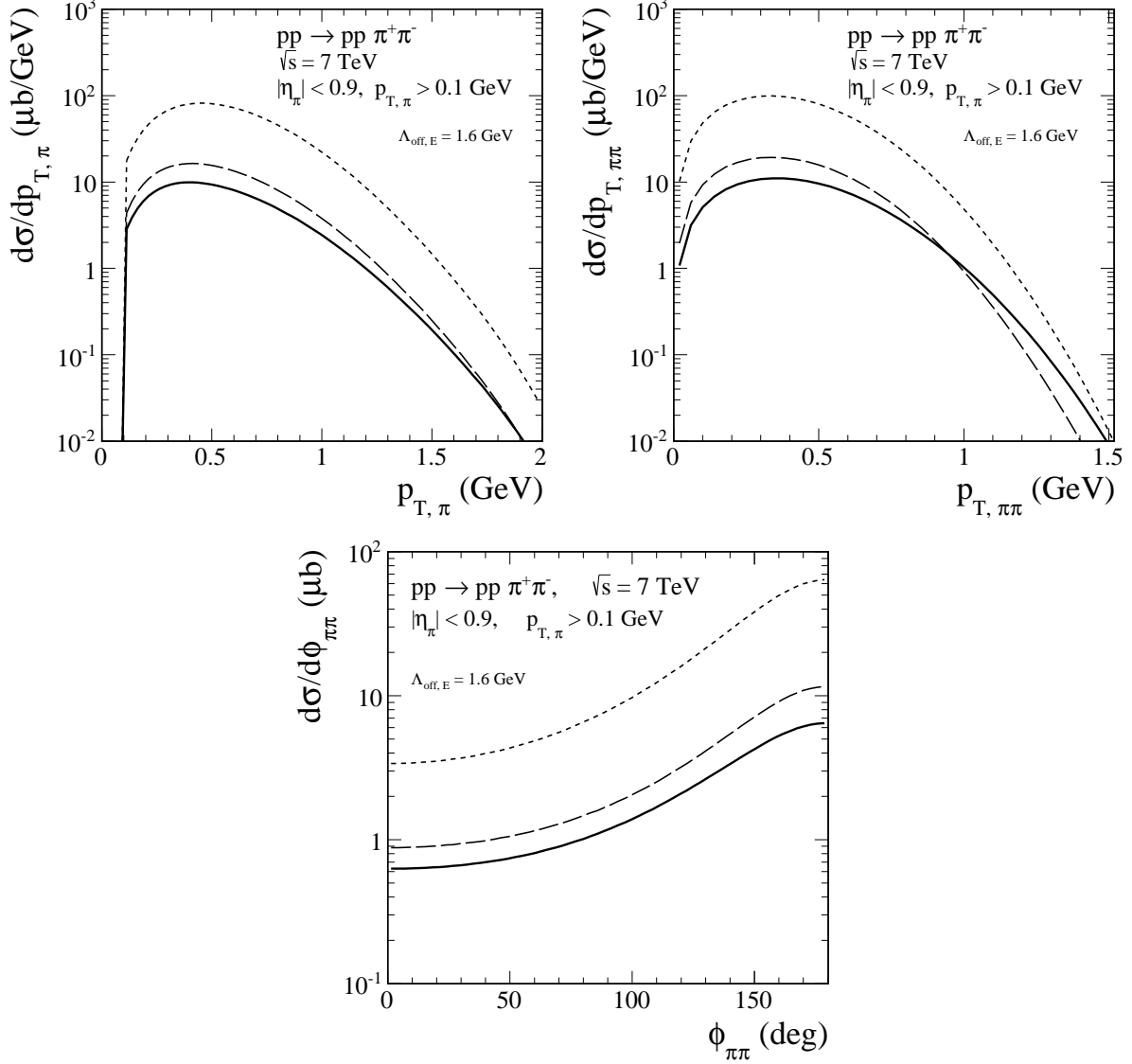


FIG. 11: Differential cross sections  $d\sigma/dp_{T,\pi}$ ,  $d\sigma/dp_{T,\pi\pi}$ , and  $d\sigma/d\phi_{\pi\pi}$  at  $\sqrt{s} = 7$  TeV with the ALICE kinematical cuts specified in the figure caption. In the calculation we have used the cut-off parameter  $\Lambda_{off,E} = 1.6$  GeV. The meaning of the lines is the same as in Fig. 5 (left panel).

extra absorption effects lead to significant modification of the shape of proton-proton relative azimuthal angle distributions which also could be tested by the two experiments.<sup>4</sup> The distributions in proton four-momentum transfer  $t = t_1 = t_2$  are presented in Fig. 14 (bottom panels). The extra pion-proton interaction increases the distribution at large  $|t|$ .

The effect of absorption can be even better seen in two-dimensional distributions in proton-proton relative azimuthal angle and transverse momentum of one of the protons,

<sup>4</sup> Note that in the case of the ATLAS experiment the requirement of both protons being tagged in the ALFA detectors influences the shapes of the distributions only very little, but it reduces the cross section by a factor close to 3 [11].

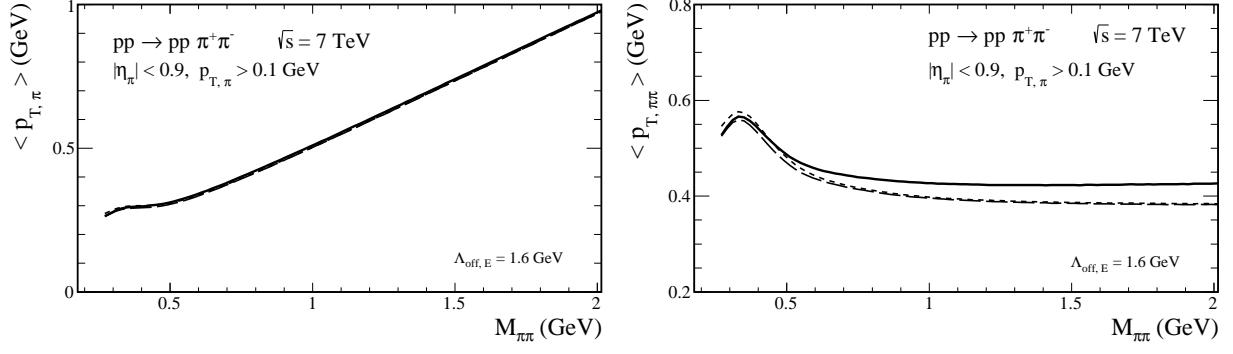


FIG. 12: Mean value of the  $p_{t,\pi}$  (left panel) and  $p_{t,\pi\pi}$  (right panel) as a function of two-pion invariant mass at  $\sqrt{s} = 7$  TeV with the ALICE kinematical cuts specified in the figure caption. In the calculation we have used the cut-off parameter  $\Lambda_{off,E} = 1.6$  GeV. The meaning of the lines is the same as in Fig. 11.

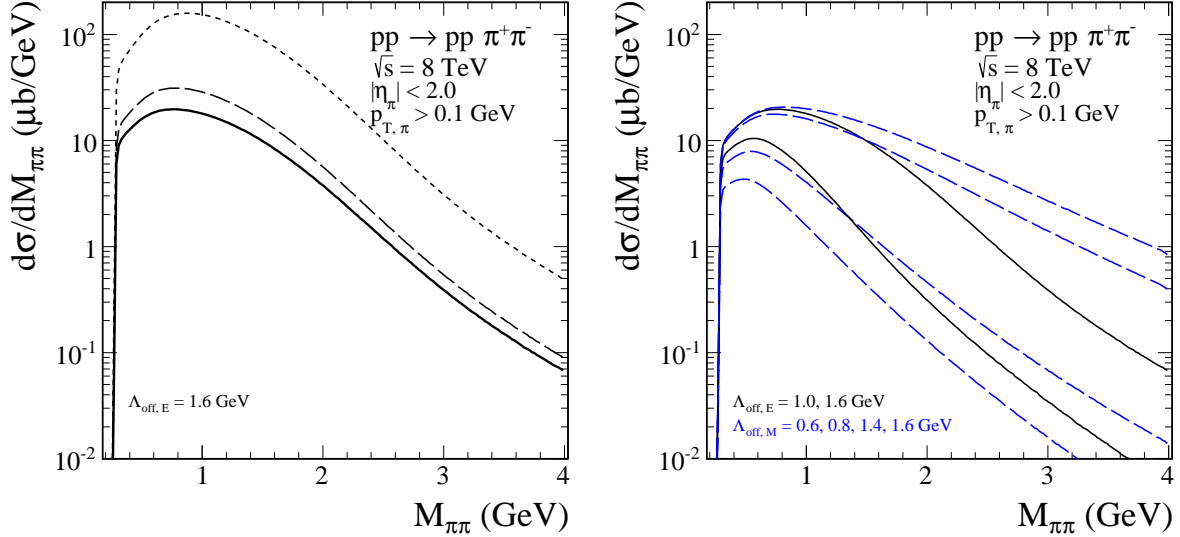


FIG. 13: Two-pion invariant mass distribution at  $\sqrt{s} = 8$  TeV with the CMS kinematical cuts specified in the figure caption. The meaning of the lines is the same as in Fig. 5.

see 15). Quite different pattern can be seen for the Born case and for the case with full absorption. It is not clear to us whether such a two-dimensional distribution can be obtained in practice.

In Table I we have collected cross sections in  $\mu b$  for the exclusive  $\pi^+\pi^-$  production with absorption effects discussed in section III and for some kinematical cuts specified in section IV. The Born cross sections for  $\sqrt{s} = 0.2, 1.96, 7, 8$  TeV and  $\Lambda_{off,E} = 1.6$  GeV are 1.13, 39.60, 54.71, 192.49  $\mu b$ , respectively. Thus the ratio of full and Born cross sections  $\langle S^2 \rangle$  (the gap survival factor) is approximately 0.20 (STAR), 0.09 (CDF), 0.12 (LHC). Results at  $\sqrt{s} = 13$  TeV were obtained also with the CMS kinematical cuts.



TABLE I: The integrated cross sections in  $\mu b$  for the central exclusive  $\pi^+\pi^-$  production via the double-pomeron/ $f_{2R}$  exchange mechanism including the  $NN$  and  $\pi N$  absorption effects. The results for different experiments with cuts specified in section IV and for the different values of the off-shell-pion form-factor parameters in Eqs. (2.12) and (2.13) are shown.

$\sqrt{s}$ (TeV):	0.2	1.96	7	8	13
$\Lambda_{off,E} = 1.6$ GeV	0.23	3.69	6.57	23.92	28.64
$\Lambda_{off,E} = 1.0$ GeV	0.09	0.63	2.16	7.88	8.98
$\Lambda_{off,M} = 1.6$ GeV	0.26	6.45	9.12	33.60	40.92
$\Lambda_{off,M} = 0.8$ GeV	0.07	0.58	1.74	6.48	7.45

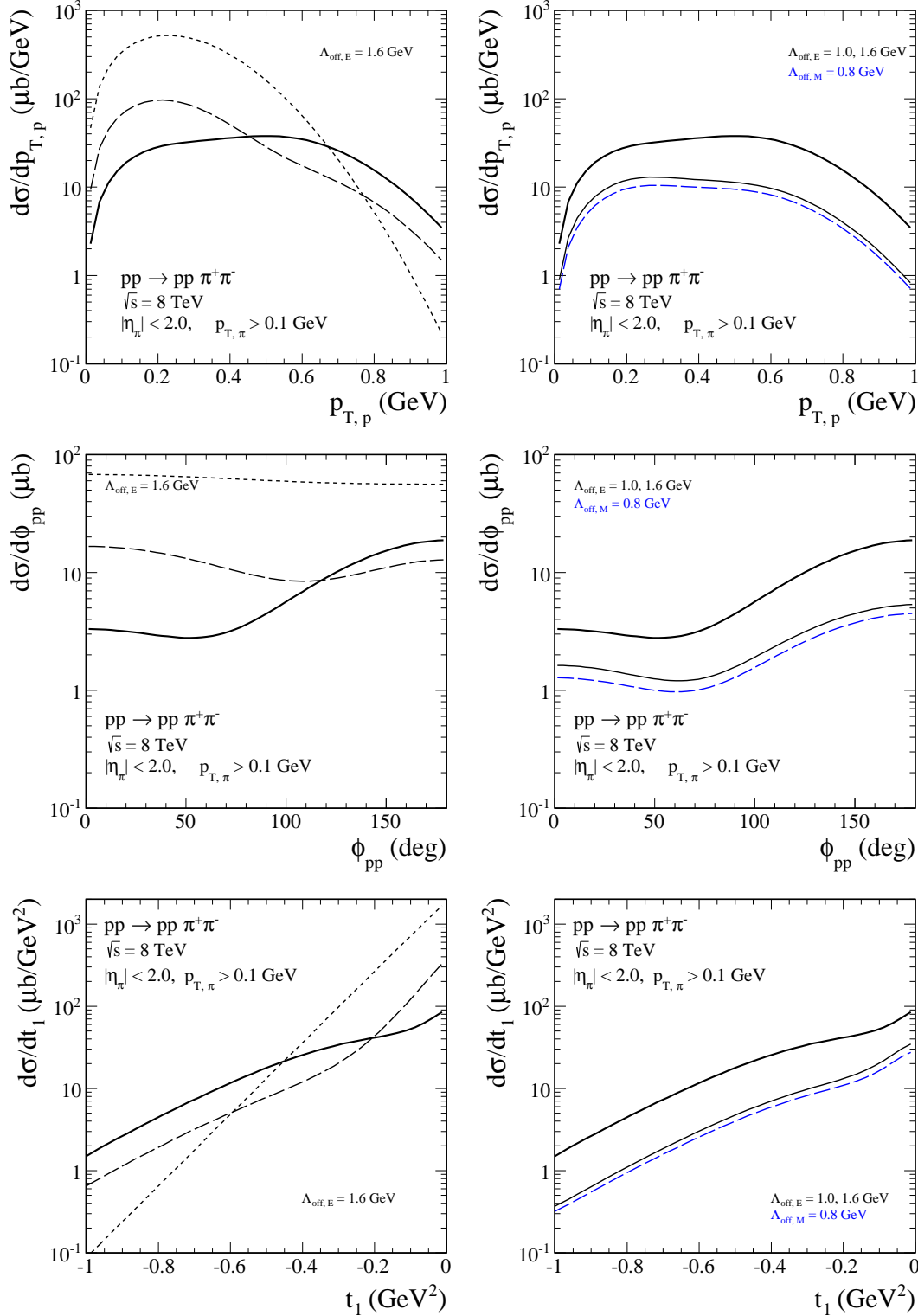


FIG. 14: The distributions in proton transverse momentum (top panels), in azimuthal angle between the outgoing protons (middle panels), and in proton four-momentum transfer  $t_1$  (bottom panels) at  $\sqrt{s} = 8$  TeV with the CMS kinematical cuts specified in the figure caption. In the left panels we show the distributions without and with the absorption corrections. In the calculation results of which are shown on the right panel we have used two form for the off-shell pion form factors and different cut-off parameters  $\Lambda_{off}$ .

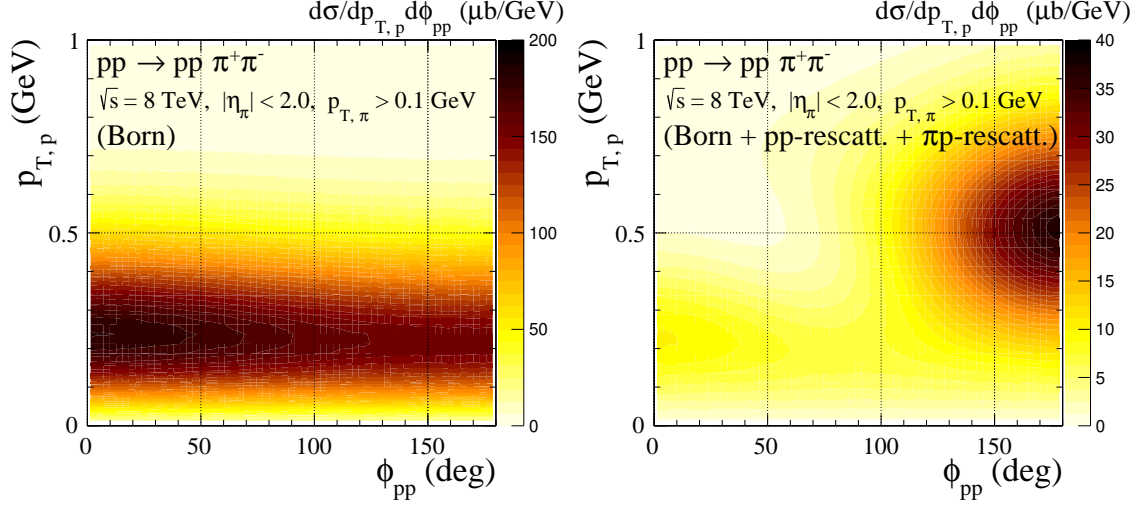


FIG. 15: Two dimensional distributions in  $p_{t,p}$  and  $\phi_{pp}$  at  $\sqrt{s} = 8 \text{ TeV}$  with the CMS kinematical cuts specified in the figure caption. We show the distributions without and with the absorption corrections. In the calculation we have used the cut-off parameter  $\Lambda_{off,E} = 1.6 \text{ GeV}$ .

## V. CONCLUSIONS

In the present paper we have taken into account absorption corrections due to pion-nucleon final state interaction in addition to those due to proton-proton interactions. To make realistic predictions of the cross sections the parameter responsible for off-shellness of intermediate pions in the Lebedowicz-Szczurek model has been adjusted to experimental data. We have considered here two different scenarios:

- 1) The parameters have been adjusted to the STAR data [6], where protons have been registered, which guarantees exclusivity of the process, however, the statistics was rather low and only low dipion invariant masses ( $M_{\pi\pi} < 1.5$  GeV) could be observed.
- 2) The parameters have been adjusted to the CDF data [8] (see also [7]), where only some rapidity gaps outside of the main detector was imposed in the experiment.

The cross section for the invariant masses  $M_{\pi\pi} < 1$  GeV is subjected to low-energy pion-pion final state interaction ( $\pi\pi$  FSI) effects which are not included in the present analysis. Thus, in the first scenario, one finds rather large  $\Lambda_{off} \approx 1.6$  GeV in the region of  $M_{\pi\pi} < 1$  GeV. In the second scenario, when the CDF data are fitted in the broad range of  $M_{\pi\pi}$  one obtains  $\Lambda_{off} \approx 0.8$  GeV. Then as a consequence one underestimates the RHIC data at  $M_{\pi\pi} \sim 0.5 - 1.0$  GeV. But this missing strength at low  $M_{\pi\pi}$  is probably due to the  $\pi\pi$  FSI enhancement in the  $\sigma$  meson region, see [43, 44]. Therefore, we might expected that at higher masses the non-resonant model (with no reggeization of intermediate pion) gives realistic predictions with the off-shell pion parameter  $\Lambda_{off} \approx 1.0$  GeV. We have proposed to use a 'stretched exponential' parametrization of  $\pi N$  amplitudes which better describes the large- $t$  region and coincides with the exponential parametrization in small- $t$  region. Such a parametrization is more adequate when focussing on larger transverse momenta. However, we fail to describe the CDF data with  $p_{t,\pi\pi} > 1$  GeV. Clearly final tuning of the model requires to take into account both  $\pi\pi$  FSI effects as well as explicit resonances such as the tensor  $f_2(1270)$  meson. This goes beyond the scope of the present paper, where we have concentrated on the absorption effects. This will be a subject of our future studies.

However, even the present rather simplified treatment of the reaction mechanism allows to draw interesting conclusions as far as the absorption effects are considered. The inclusion of the pion-nucleon interactions lead to additional damping of the cross section by a factor of about 2, almost independent of center-of-mass energy at least in the range considered in the present paper. The additional interaction changes the shape of some distributions ( $d\sigma/dt_{1/2}$ ,  $d\sigma/dp_{t,p}$ ,  $d\sigma/d\phi_{pp}$ ) but leaves almost unchanged shape of other distributions ( $d\sigma/dM_{\pi\pi}$ ,  $d\sigma/dy_\pi$ ,  $d\sigma/dp_{t,\pi}$ ,  $d\sigma/d\phi_{\pi\pi}$ ). Particularly spectacular modifications are obtained for  $|t|$  and  $p_{t,p}$  distributions. In particular, a measurement of the distribution in the relative azimuthal angle between the  $p_t$  vectors of the outgoing protons can provide a fully differential test of the soft survival factors. This could be verified in future in experiments when both protons are measured such as ATLAS + ALFA [11] or CMS + TOTEM [12]. In summary, the additional absorption effect discussed here seems crucial in detailed understanding of results of ongoing and planned experimental investigations.

## Acknowledgments

We are indebted to Mike Albrow, Lidia Görlich, Valery Khoze, Wolfgang Schäfer, Reiner Schicker, and Jacek Turnau for interesting discussions. We are grateful to Maria Żurek for sending us the recent CDF data points. The work of P.L. was supported by the NCN Grant No. DEC-2013/08/T/ST2/00165, the MNiSW Grant No. IP2014 025173 “Juventus Plus” and by the START fellowship from the Foundation for Polish Science. The work of A.S. was partially supported by the Centre for Innovation and Transfer of Natural Sciences and Engineering Knowledge in Rzeszów.

- 
- [1] M. G. Albrow, T. D. Coughlin, and J. R. Forshaw, *Central exclusive particle production at high energy hadron colliders*, Prog.Part.Nucl.Phys. **65** (2010) 149–184, arXiv:1006.1289 [hep-ph].
  - [2] P. Lebiedowicz, *Exclusive reactions with light mesons: From low to high energies*. PhD thesis, IFJ PAN, 2014. The thesis is available at [http://www.ifj.edu.pl/msd/rozprawy\\_dr/rozpr\\_Lebiedowicz.pdf](http://www.ifj.edu.pl/msd/rozprawy_dr/rozpr_Lebiedowicz.pdf).
  - [3] M. Albrow, *Central exclusive production issue: Introduction*, Int.J.Mod.Phys. **A29** (2014) 1402006.
  - [4] A. Austregesilo, (COMPASS Collaboration), *A Partial-Wave Analysis of Centrally Produced Two-Pseudoscalar Final States in pp Reactions at COMPASS*, PoS **Bormio2013** (2013) 014.
  - [5] A. Austregesilo, *Central Production of Two-Pseudoscalar Meson Systems at the COMPASS Experiment at CERN*, CERN-THESIS-2014-190.
  - [6] L. Adamczyk, W. Guryn, and J. Turnau, *Central exclusive production at RHIC*, Int.J.Mod.Phys. **A29** no. 28, (2014) 1446010, arXiv:1410.5752 [hep-ex].
  - [7] M. Albrow, J. Lewis, M. Żurek, A. Święch, D. Lontkovskyi, I. Makarenko, and J. S. Wilson. The public note called *Measurement of Central Exclusive Hadron Pair Production in CDF* is available at [http://www-cdf.fnal.gov/physics/new/qcd/GXG\\_14/webpage/](http://www-cdf.fnal.gov/physics/new/qcd/GXG_14/webpage/).
  - [8] T. A. Aaltonen *et al.*, (CDF Collaboration), *Measurement of central exclusive  $\pi^+\pi^-$  production in  $p\bar{p}$  collisions at  $\sqrt{s} = 0.9$  and 1.96 TeV at CDF*, arXiv:1502.01391 [hep-ex].
  - [9] R. Schicker, (ALICE Collaboration), *Central Diffraction in ALICE*, arXiv:1205.2588 [hep-ex].
  - [10] R. Schicker, *Diffraction production of mesons*, arXiv:1410.6060 [hep-ph].
  - [11] R. Staszewski, P. Lebiedowicz, M. Trzebiński, J. Chwastowski, and A. Szczurek, *Exclusive  $\pi^+\pi^-$  Production at the LHC with Forward Proton Tagging*, Acta Phys.Polon. **B42** (2011) 1861–1870, arXiv:1104.3568 [hep-ex].
  - [12] K. Österberg, *Potential of central exclusive production studies in high  $\beta^*$  runs at the LHC with CMS-TOTEM*, Int.J.Mod.Phys. **A29** no. 28, (2014) 1446019.
  - [13] A. Szczurek and P. Lebiedowicz, *Exclusive scalar  $f_0(1500)$  meson production for energy ranges available at the GSI Facility for Antiproton and Ion Research (GSI-FAIR) and at the Japan Proton Accelerator Research Complex (J-PARC)*, Nucl.Phys. **A826** (2009) 101–130, arXiv:0906.0286 [nucl-th].
  - [14] W. Ochs, *The Status of Glueballs*, J.Phys. **G40** (2013) 043001, arXiv:1301.5183 [hep-ph].
  - [15] A. Kirk, *A review of central production experiments at the CERN Omega spectrometer*, Int.J.Mod.Phys. **A29** no. 28, (2014) 1446001, arXiv:1408.1196 [hep-ex].
  - [16] C. Ewerz, M. Maniatis, and O. Nachtmann, *A Model for Soft High-Energy Scattering: Tensor Pomeron and Vector Odderon*, Annals of Physics **342** (2014) 31–77, arXiv:1309.3478 [hep-ph].
  - [17] P. Lebiedowicz, O. Nachtmann, and A. Szczurek, *Exclusive central diffractive production of scalar and pseudoscalar mesons; tensorial vs. vectorial pomeron*, Annals Phys. **344** (2014) 301–339, arXiv:1309.3913 [hep-ph].
  - [18] P. Lebiedowicz, O. Nachtmann, and A. Szczurek,  *$\rho^0$  and Drell-Söding contributions to central exclusive production of  $\pi^+\pi^-$  pairs in proton-proton collisions at high energies*, Phys.Rev. **D91** no. 7, (2015) 074023, arXiv:1412.3677 [hep-ph].
  - [19] P. Lebiedowicz, R. Pasechnik, and A. Szczurek, *Measurement of exclusive production of scalar  $\chi_{c0}$  meson in proton-(anti)proton collisions via  $\chi_{c0} \rightarrow \pi^+\pi^-$  decay*, Phys.Lett. **B701** (2011) 434–444, arXiv:1103.5642 [hep-ph].

- [20] L. A. Harland-Lang, V. A. Khoze, M. G. Ryskin, and W. J. Stirling, *The Phenomenology of Central Exclusive Production at Hadron Colliders*, Eur.Phys.J. **C72** (2012) 2110, arXiv:1204.4803 [hep-ph].
- [21] P. Lebiedowicz and A. Szczurek, *Exclusive  $pp \rightarrow nn\pi^+\pi^+$  reaction at LHC and RHIC*, Phys.Rev. **D83** (2011) 076002, arXiv:1005.2309 [hep-ph].
- [22] A. Cisek, P. Lebiedowicz, W. Schäfer, and A. Szczurek, *Exclusive production of  $\omega$  meson in proton-proton collisions at high energies*, Phys.Rev. **D83** (2011) 114004, arXiv:1101.4874 [hep-ph].
- [23] P. Lebiedowicz and A. Szczurek, *Exclusive  $pp \rightarrow pp\pi^0$  reaction at high energies*, Phys.Rev. **D87** (2013) 074037, arXiv:1303.2882 [hep-ph].
- [24] P. Lebiedowicz and A. Szczurek, *Exclusive  $pp \rightarrow pp\pi^+\pi^-$  reaction: From the threshold to LHC*, Phys.Rev. **D81** (2010) 036003, arXiv:0912.0190 [hep-ph].
- [25] R. Waldi, K. R. Schubert, and K. Winter, *Search for glueballs in a pomeron pomeron scattering experiment*, Z.Phys. **C18** (1983) 301–306.
- [26] A. Breakstone *et al.*, (ABCDHW Collaboration), *Inclusive Pomeron-Pomeron Interactions at the CERN ISR*, Z.Phys. **C42** (1989) 387.
- [27] A. Breakstone *et al.*, (ABCDHW Collaboration), *The reaction Pomeron-Pomeron  $\rightarrow \pi^+\pi^-$  and an unusual production mechanism for the  $f_2(1270)$* , Z.Phys. **C48** (1990) 569–576.
- [28] R. Kycia, J. Chwastowski, R. Staszewski, and J. Turnau, *GenEx: A simple generator structure for exclusive processes in high energy collisions*, arXiv:1411.6035 [hep-ph].
- [29] L. A. Harland-Lang, V. A. Khoze, and M. G. Ryskin, *Modelling exclusive meson pair production at hadron colliders*, Eur.Phys.J. **C74** (2014) 2848, arXiv:1312.4553 [hep-ph].
- [30] A. Donnachie, H. G. Dosch, P. V. Landshoff, and O. Nachtmann, *Pomeron physics and QCD*, Camb.Monogr.Part.Phys.Nucl.Phys.Cosmol. **19** (2002) 1–347.
- [31] A. Donnachie and P. V. Landshoff,  *$pp$  and  $\bar{p}p$  total cross sections and elastic scattering*, MAN-HEP-2013-19-DAMTP-2013-38, arXiv:1309.1292 [hep-ph].
- [32] M. G. Ryskin, A. D. Martin, and V. A. Khoze, *High-energy strong interactions: from ‘hard’ to ‘soft’*, Eur.Phys.J. **C71** (2011) 1617, arXiv:1102.2844 [hep-ph].
- [33] S. Fazio, R. Fiore, L. Jenkovszky, and A. Sali, *Unifying ‘soft’ and ‘hard’ diffractive exclusive vector meson production and deeply virtual Compton scattering*, Phys.Rev. **D90** no. 1, (2014) 016007, arXiv:1312.5683 [hep-ph].
- [34] L. L. Jenkovszky, A. I. Lengyel, and D. I. Lontkovskiy, *The Pomeron and Odderon in elastic, inelastic and total cross sections at the LHC*, Int.J.Mod.Phys. **A26** (2011) 4755–4771, arXiv:1105.1202 [hep-ph].
- [35] V. A. Khoze, A. D. Martin, and M. G. Ryskin,  *$t$  dependence of the slope of the high energy elastic  $pp$  cross section*, J.Phys. **G42** no. 2, (2015) 025003, arXiv:1410.0508 [hep-ph].
- [36] A. Cisek, W. Schäfer, and A. Szczurek, *Exclusive photoproduction of charmonia in  $\gamma p \rightarrow Vp$  and  $pp \rightarrow pVp$  reactions within  $k_t$ -factorization approach*, JHEP **1504** (2015) 159, arXiv:1405.2253 [hep-ph].
- [37] J. Orear, *Transverse Momentum Distribution of Protons in  $p$ - $p$  Elastic Scattering*, Phys.Rev.Lett. **12** (1964) 112–113.
- [38] C. W. Akerlof, R. Kotthaus, R. L. Loveless, D. I. Meyer, I. Ambats, *et al.*, *Hadron-Proton Elastic Scattering at 50 GeV/c, 100 GeV/c and 200 GeV/c Momentum*, Phys.Rev. **D14** (1976) 2864.
- [39] D. S. Ayres *et al.*, (Fermilab Single Arm Spectrometer Group),  *$\pi^\pm p$ ,  $K^\pm p$ ,  $pp$  and  $\bar{p}p$  Elastic Scattering from 50 GeV/c to 175 GeV/c*, Phys.Rev. **D15** (1977) 3105.
- [40] Z. Asa’d *et al.*, (Annecy(LAPP)-CERN-Bohr Inst-Genoa-Oslo-London), *Elastic Scattering of*

- charged mesons, antiprotons and protons on protons at incident momenta of 20, 30 and 50 GeV/c in the momentum transfer range  $0.5 < -t < 8 \text{ (GeV/c)}^2$ , Nucl.Phys. **B255** (1985) 273.*
- [41] A. Schiz, L. A. Fajardo, R. Majka, J. N. Marx, P. Nemethy, *et al.*, *A High Statistics Study of  $\pi^+ p$ ,  $\pi^- p$ , and  $pp$  Elastic Scattering at 200 GeV/c*, Phys.Rev. **D24** (1981) 26.
  - [42] R. Rubinstein, W. Baker, D. P. Eartly, J. Klinger, A. J. Lennox, *et al.*, *Large-momentum-transfer elastic scattering of  $\pi^\pm$ ,  $K^\pm$ , and  $p^\pm$  on protons at 100 and 200 GeV/c*, Phys.Rev. **D30** (1984) 1413.
  - [43] J. Pumplin and F. S. Henyey, *Double Pomeron Exchange in the Reaction  $pp \rightarrow pp\pi^+\pi^-$* , Nucl.Phys. **B117** (1976) 377–396.
  - [44] K. L. Au, D. Morgan, and M. R. Pennington, *Meson Dynamics Beyond the Quark Model: A Study of Final State Interactions*, Phys.Rev. **D35** (1987) 1633.